A FAST INTEGRATED GREEN FUNCTION METHOD FOR COMPUTING 1D CSR WAKEFIELDS INCLUDING UPSTREAM TRANSIENTS

C.E. Mitchell, Ji Qiang, and R.D. Ryne, Lawrence Berkeley National Laboratory, USA

Abstract

An efficient numerical method for computing wakefields due to coherent synchrotron radiation (CSR) has been implemented using a one-dimensional integrated Green function approach. The contribution from CSR that is generated upstream and propagates across one or more lattice elements before interacting with the bunch is included. This method does not require computing the derivative of the longitudinal charge density, and accurately includes the short-range behavior of the CSR interaction. As an application of this method, we examine the importance of upstream transient wakefields within several bending elements of a proposed Next Generation Light Source.

BACKGROUND

The accurate modeling of coherent synchrotron radiation is a numerical challenge of key importance to the development of future light sources [1]. Recent 3D simulations of the CSR generated by Gaussian bunches of various shapes [2] confirm that a 1D model of the longitudinal CSR wakefield is accurate provided that the transverse rms beam size $\sigma_\perp$ satisfies $\sigma_\perp << R(\sigma_z/R)^{2/3}$, where R is the bending radius and σ_z is the longitudinal rms beam size. A number of such 1D models appear in the literature [3]–[7], many of which have been implemented in existing beam dynamics codes.

In these models, the energy loss per unit length at a longitudinal location z within the bunch is given by:

$$W(z) = \int_{-\infty}^{z} \lambda(z') K_{CSR}(z, z') dz', \qquad (1)$$

where λ is the longitudinal number density of the bunch, and K_{CSR} is related to the longitudinal component of the Liénard-Wiechert field $\mathbf{E}^{LW}$ of a single particle [6]. The integration kernel K_{CSR} varies rapidly near $z \approx z'$ on the scale $R/\gamma^3 << \sigma_z$, and the integral (1) is therefore difficult to resolve numerically. This problem is typically avoided by computing the equivalent integral

$$W(z) = \int_{-\infty}^{z} \frac{d\lambda(z')}{dz'} I_{CSR}(z, z') dz', \qquad (2)$$

where

$$I_{CSR}(z, z') = -\int_{-\infty}^{z'} K_{CSR}(z, z'') dz''. \qquad (3)$$

The kernel I_{CSR} exhibits less singular behavior than K_{CSR} near $z \approx z'$. However, this method requires that one evaluate the numerical derivative of the longitudinal charge density, which in general contains significant numerical noise. It is also typical to approximate I_{CSR} by an asymptotic form. (See, for example, equation (19) of [4].)

In the following section, we describe an efficient method for evaluating (1) that makes use of the longitudinal charge density λ directly. The short-range behavior of the CSR kernel is treated analytically, so that only longitudinal variations in the charge density need to be resolved [8, 9]. In addition, this method can be used to treat the case of entry and exit transient fields [4], as well as the case of transient fields in a general lattice due to upstream elements [6].

INTEGRATED GREEN FUNCTION METHODS

Let $\lambda_j = \lambda(z_j)$, $j = 1, \ldots, N$ denote the values of the longitudinal number density of the bunch at a set of equidistant sample points z_j, $j = 1, \ldots, N$, and let $\{P_j : j = 1, \ldots, N\}$ denote a basis of piecewise polynomials of given degree. This basis can always be chosen such that $P_j(z_k) = \delta_{j,k}$. We can then write the interpolated longitudinal density $\lambda_{appx} \approx \lambda$ in the form

$$\lambda_{appx} = \sum_{j=1}^{N} \lambda_j P_j(z). \qquad (4)$$

Using (4) in (1) gives an approximate longitudinal wakefield $W_{approx} \approx W$ of the form

$$W_{approx}(z_k) = \sum_{k'=1}^{N} \lambda_{k'} w_{k,k'}, \quad \text{where} \qquad (5)$$

$$w_{k,k'} = \int_{-\infty}^{z_k} P_{k'}(z') K_{CSR}(z_k, z') dz'.$$

For the models described in [3]–[6], the weights $w_{k,k'}$ may be determined analytically in terms of rational functions, log, arctan, and polynomial roots. In particular, the quantities $w_{k,k'}$ have been determined explicitly for the 1D models described in [4, 6] in the cases of both piecewise constant and piecewise linear basis functions.

For example, a set of piecewise-constant basis functions is given, for stepsize h, by:

$$P_{k'}(z) = \begin{cases} 1, & z_{k'} - h/2 \le z \le z_{k'} + h/2, \\ 0, & \text{else} \end{cases} \qquad (6)$$

when $1 < k' < k$, with similar expressions for P_1 and P_k.

We then have for $1 \le k \le N$:

$$w_{k,k'} = I_{CSR}\left(z_k, z_{k'} - \frac{h}{2}\right) - I_{CSR}\left(z_k, z_{k'} + \frac{h}{2}\right), \qquad (7)$$

ISBN 978-3-95450-116-8

for $1 < k' < k$ and

$$w_{k,1} = I_{CSR}\left(z_k, z_1\right) - I_{CSR}\left(z_k, z_1 + \frac{h}{2}\right), \quad (8)$$

$$w_{k,k} = I_{CSR}\left(z_k, z_k - \frac{h}{2}\right) - I_{CSR}\left(z_k, z_k\right). \quad (9)$$

For the four cases considered in [4], the function I_{CSR} is given in Cases A–D, respectively, by the expressions:

$$\frac{RI_{CSR}}{\gamma r_c mc^2} = -\frac{2(\hat{\phi}+\hat{y}) + \hat{\phi}^3}{(\hat{\phi}+\hat{y})^2 + \hat{\phi}^4/4} + \frac{1}{\hat{s}}, \quad (10)$$

where $\hat{s} = \dfrac{\hat{\phi}+\hat{y}}{2} + \dfrac{\hat{\phi}^3}{24}\dfrac{\hat{\phi}+4\hat{y}}{\hat{\phi}+\hat{y}}$.

$$\frac{RI_{CSR}}{\gamma r_c mc^2} = -\frac{4\hat{u}(\hat{u}^2+8)}{(\hat{u}^2+4)(\hat{u}^2+12)}, \quad (11)$$

where $\hat{s} = \dfrac{\hat{u}^3}{24} + \dfrac{\hat{u}}{2}$.

$$\frac{RI_{CSR}}{\gamma r_c mc^2} = -\frac{2(\hat{\phi}_m + \hat{x} + \hat{y} + \hat{\phi}_m^3/2 + \hat{\phi}_m^2\hat{x})}{(\hat{x}+\hat{y}+\hat{\phi}_m)^2 + (\hat{\phi}\hat{x} + \hat{\phi}_m^2/2)^2} + \frac{1}{\hat{s}}, \quad (12)$$

where $\hat{s} = \dfrac{\hat{\phi}+\hat{x}+\hat{y}}{2} + \dfrac{\hat{\phi}_m^2}{24}\dfrac{\hat{\phi}_m^2 + 4\hat{\phi}_m(\hat{x}+\hat{y}) + 12\hat{x}\hat{y}}{\hat{\phi}+\hat{x}+\hat{y}}$.

$$\frac{RI_{CSR}}{\gamma r_c mc^2} = -\frac{2(\hat{\psi} + \hat{x} + \hat{\psi}^3/2 + \hat{\psi}^2\hat{x})}{(\hat{x}+\hat{\psi})^2 + (\hat{\psi}\hat{x} + \hat{\psi}^2/2)^2} + \frac{1}{\hat{s}}, \quad (13)$$

where $\hat{s} = \dfrac{\hat{\psi}+\hat{x}}{2} + \dfrac{\hat{\psi}^2}{24}\dfrac{\hat{\psi}^2 + 4\hat{x}\hat{\psi}}{\hat{\psi}+\hat{x}}$.

The notation appearing on the right-hand side in (10–13) is the same as the notation used in [4].

It is possible to express the sum (5) in the form of a discrete convolution, which can then be evaluated using an FFT in $O(N \log N)$ operations. This technique has been implemented in the code IMPACT. A routine using the more general expression for I_{CSR} provided in [6] has also been developed, and may also be used when we wish to include transient effects due to CSR from upstream lattice elements.

NUMERICAL ANALYSIS

Several methods for computing the longitudinal wake integral (1) were compared against the integrated Green function method described in the previous section. These include:

- Direct evaluation of (1) using an extended trapezoidal rule.
- Evaluation using an integrated Green function method with piecewise constant basis functions.
- Evaluation using an integrated Green function method with piecewise linear basis functions.
- Evaluation of (2) using an extended trapezoidal rule, when $d\lambda/dz$ is exactly known.
- Evaluation of (2) using an extended trapezoidal rule, when $d\lambda/dz$ is approximated using a central difference formula.

These methods share the property that the local error on each subinterval scales as $O(h^3)$. Figure 1 illustrates the relative error in the value of the CSR wake computed at the centroid of a Gaussian bunch as a function of stepsize, for the five algorithms above. Note that the convergence behavior of the direct integration method changes near $h = R/\gamma^3$ (indicated by the vertical dashed line). When this scale is not resolved, this method has an error that is a factor of $10^5 - 10^6$ worse than the other methods considered here. The figure below shows the error in the region $h \geq R/\gamma^3$, indicating that the IGF method with a piecewise constant basis results in the smallest error over a large range of stepsizes.

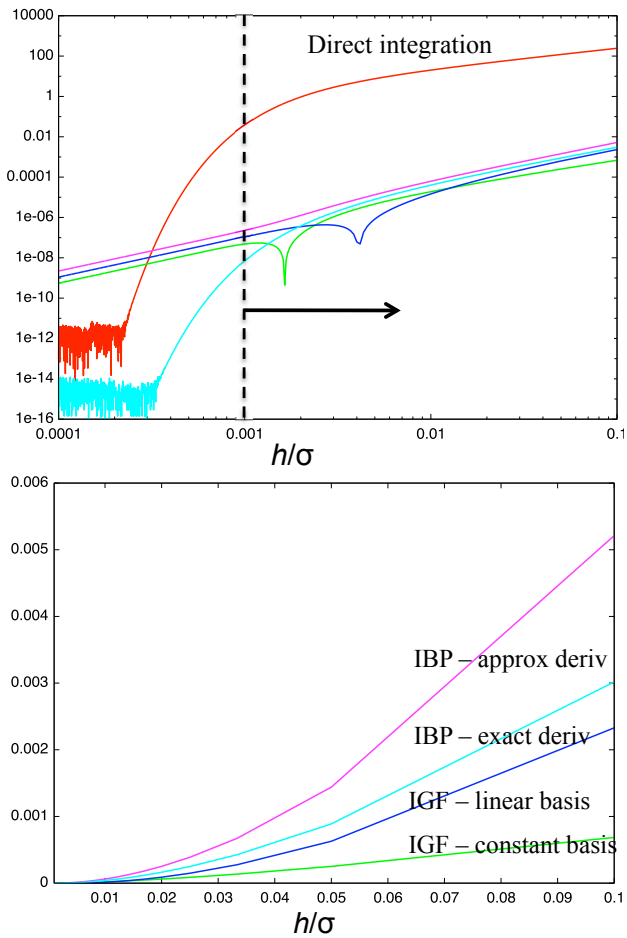

Figure 1: (Upper) Relative error in the computed longitudinal CSR wake at $z = 0$ for a Gaussian bunch with $\sigma = 0.1$ mm at 200 MeV in a bend with $R = 10$ m. The result is shown for 5 distinct quadrature formulas as a function of stepsize (log-log scale). (Lower) The same quantities shown on a linear scale for $h \geq R/\gamma^3$.

ISBN 978-3-95450-116-8

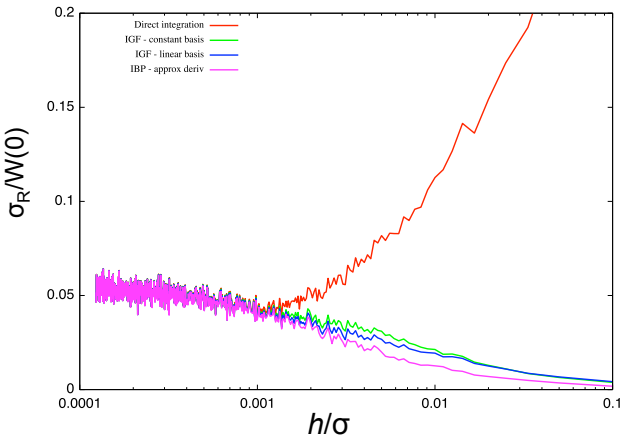

Figure 2: Sensitivity to noise in the CSR wake at $z = 0$ for a Gaussian bunch for 5 distinct quadrature formulas, shown as a function of stepsize (log-linear scale). Colors have the same meaning as in the previous figure. The shot noise (14) at a given step size h is determined by the two parameters $N = 20\sigma/h$ and $N_p = 10^6$.

The values λ_j are in general obtained by projecting a distribution of N_p macroparticles into N longitudinal bins, therefore introducing shot noise to the longitudinal density profile of the beam. We model this noise by setting

$$\lambda_j^r = \lambda_j(1 + \epsilon_j), \quad j = 1, \ldots, N, \tag{14}$$

where each ϵ_j is a normal random variable with $\langle \epsilon_j \rangle = 0$ and $\langle \epsilon_j^2 \rangle = N/N_p$. The CSR wake may now be computed using either the smooth values λ_j or the noisy values λ_j^r. We refer to the difference between these two results as the *sensitivity to noise*. The rms value of the sensitivity to noise at the centroid of a Gaussian bunch is shown in Fig. 2 for the five algorithms described above. Each value was obtained by averaging over 100 distinct random seeds. Note that the direct integration method (red) is very sensitive to the presence of noise, while the other methods exhibit sensitivities that are comparable to one another.

APPLICATION TO NGLS

The integrated Green function method of (5) was used to study longitudinal CSR wakefields in the spreader section of a proposed Next Generation Light Source [1]. The 2.4 GeV spreader section directs the beam bunches into several parallel FEL lines using a series of six 10° dipoles. The CSR wake was computed inside Bend 6 (Fig. 3) using the model of [6] with piecewise constant basis functions. Figure 4 illustrates an analytical model of the current pulse at the spreader entry, together with the upstream contribution of Bends 4 and 5 to the longitudinal wakefield at several locations within Bend 6. After computing the net energy kick experienced by particles in the bunch as they propagate through the spreader dipoles, the CSR from upstream bends was found to contribute 12% of the total energy kick in the spreader.

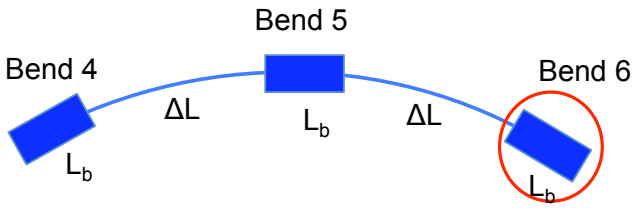

Figure 3: The final 3 dipoles appearing in the spreader section of a Next Generation Light Source. The longitudinal CSR wake was computed in Bend 6 both with and without the effects of radiation from Bends 4 and 5 included.

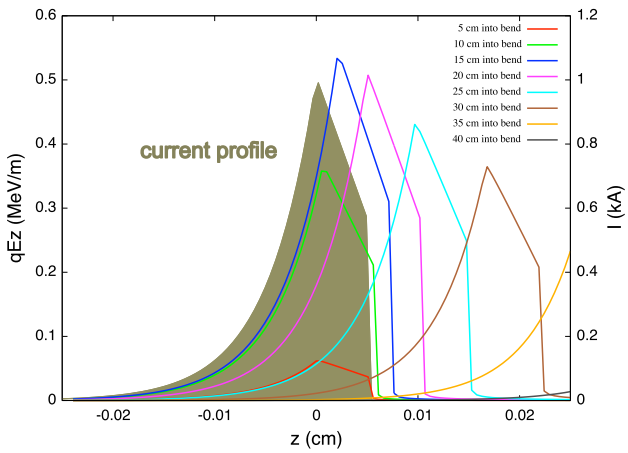

Figure 4: (Brown) Model of the current pulse entering the NGLS spreader. (Curves) The difference between the longitudinal CSR wakefield in Bend 6 when computed with and without the effects of the upstream bends 4 and 5, shown at distances of 5–40 cm into the bend.

CONCLUSIONS

A one-dimensional integrated Green function method using both a piecewise constant and a piecewise linear basis has been implemented to model longitudinal CSR wakefields using the models described in [4, 6]. This method does not require computing the derivative of the longitudinal charge density, and accurately includes the short-range behavior of the CSR interaction. The error is smaller than other methods which have a comparable rate of convergence. As an application of this method, we studied upstream transient wakefields within the spreader section of a proposed Next Generation Light Source.

ACKNOWLEDGEMENT

This work is supported by the Office of Science of the U.S. Department of Energy under Contract No. DE-AC02-05CH11231.

ISBN 978-3-95450-116-8

REFERENCES

[1] John Corlett et al., "Next Generation Light Source R& D and Design Studies at LBNL", to appear in Proc. of IPAC 2012.

[2] R.D. Ryne et al, Proc. IPAC 2012, New Orleans, Lousiana, 1689 (2012).

[3] J. Murphy et al, Particle Accelerators, **57**, pp. 9–64 (1997).

[4] E.L. Saldin et al., Nucl. Instrum. Methods Phys. Res. A **398**, 373 (1997).

[5] G. Stupakov and P. Emma, Proc. EPAC 2002, Paris, France, 1479 (2002).

[6] D. Sagan et al., Phys. Rev. ST - Accel. Beams **12**, 040703 (2009).

[7] C. Mayes and G. Hoffstaetter, Phys. Rev. ST - Accel. Beams **12**, 024401 (2009).

[8] R.D. Ryne et al., `http://arxiv.org/abs/1202.2409` (2012).

[9] Ji Qiang et al., Nucl. Instrum. Methods Phys. Res. A **682**, 49–53 (2012).

ISBN 978-3-95450-116-8